Structural imaging of surface oxidation and oxidation catalysis on Ru(0001)

J. I. Flege,[1] J. Hrbek,[1,2] and P. Sutter[1]
[1]*Center for Functional Nanomaterials, Brookhaven National Laboratory, Upton, New York 11973, USA*
[2]*Department of Chemistry, Brookhaven National Laboratory, Upton, New York 11973, USA*
(Received 3 September 2008; published 7 October 2008)

Using simultaneous imaging and structural fingerprinting under reaction conditions, we probe the initial oxidation pathway and CO oxidation catalysis on Ru(0001). Oxidation beyond an initial (1×1)-O adlayer phase produces a heterogeneous surface, comprising a disordered trilayerlike surface oxide and an ordered $RuO_2(110)$ thin-film oxide, which form independently and exhibit similar stability. The surface oxide and RuO_2 phases both show high intrinsic catalytic activity. The oxygen adlayer is inactive in isolation but becomes active due to cooperative effects in close proximity to the surface oxide.

DOI: 10.1103/PhysRevB.78.165407 PACS number(s): 82.45.Jn, 68.37.Nq, 81.65.Mq, 82.40.Np

I. INTRODUCTION

The oxides of 4*d* late transition metals, such as ruthenium (Ru) and rhodium (Rh) form spontaneously under oxidizing conditions and exhibit complex functional properties, e.g., in oxidation catalysis.[1] However, the mechanism of initial oxidation of these materials and the nature of the structures produced by facile oxygen uptake into subsurface layers[2]—crucial for assessing and tailoring oxide function—have been notoriously difficult to investigate experimentally primarily because of a lack of spatially resolving and structurally sensitive techniques adequate for following the formation and conversion of nanometer-sized oxidation products under reaction conditions.

Here we use spatially and temporally resolved structural fingerprinting to characterize surface oxidation as well as the catalytic properties of the resulting oxygen-rich structures on Ru(0001). For heterogeneous (e.g., partially oxidized) surfaces, the standard approach to determining structure by surface crystallography—analysis of low-energy electron diffraction (LEED) intensities (I) as a function of the incident electron energy (V) (Ref. 3)—is hindered by the superposition of diffraction patterns with possibly very different intensities but similar lateral periodicities. This problem can be overcome by measuring the $I(V)$ characteristics in real space with sufficient resolution to isolate individual nanoscale domains; a concept realized in *IV* low-energy electron microscopy (*IV*-LEEM).[4] Spectroscopic stacks of images of a surface are acquired from the (00) diffraction beam as a function of electron energy, V, so that the local image intensity, $I(x,y;V)$, represents the specular low-energy electron reflectivity of nanoscale surface areas. From a time-lapse sequence of such stacks time-dependent $I(V)$ spectra can be obtained at every image pixel. When combined with dynamical multiple-scattering calculations of the low-energy electron reflectivity,[5] this information can be used for structural fingerprinting and to track nanoscale near-surface phases as they evolve and transform into one another.

We use *IV*-LEEM to examine the initial oxidation of Ru(0001), which has remained unexplained despite intense theoretical and experimental efforts. Ru(0001) oxidation was predicted to involve a surface oxide in the form of a floating O-Ru-O-O trilayer as a metastable precursor to a stable RuO_2 thin-film oxide that is structurally equivalent to the bulk oxide of Ru.[6,7] While solid experimental evidence for the existence of the trilayer and, in particular, its role in the oxidation process is still lacking for Ru(0001), similar surface oxides have been identified for other transition metals, e.g., Rh(111),[8] and appear to be a central element in the initial oxidation of this entire class of materials.

II. INITIAL STAGES OF Ru(0001) OXIDATION

In situ IV-LEEM on Ru(0001) exposed to large doses of NO_2 (7.6×10^{-4} torr s=760 Langmuir, L) at high temperature (790 K) shows three distinct surface phases [Fig. 1(a)], as characterized by their distinct $I(V)$ curves [Fig. 1(b)].[9] The surface is uniformly covered by phase (i) at low oxygen dose. Phases (ii) and (iii) nucleate and then grow at the expense of (i) during continued exposure.[10] This observation suggests that (i) is the well-known (1×1)-O adlayer phase in which the metal surface is terminated by a full monolayer (ML) of oxygen,[11] whereas (ii) and (iii) are oxygen-rich phases with local coverage $\Theta_O>1$ ML. This assignment is confirmed by comparing local $I(V)$ spectra of phase (i) with the theoretical (00) $I(V)$ characteristic of Ru(0001)-(1×1)-O calculated using LEED theory[5] and is corroborated independently by its sharp (1×1) selected-area electron diffraction (micro-LEED) pattern [Fig. 1(b)]. Using the same methodology, we have characterized the oxygen-rich phases (ii) and (iii). Stable Ru-O structures[7] predicted by density-functional theory (DFT) served as trial geometries for the $I(V)$ calculations. For the purpose of structural fingerprinting, all atomic coordinates were kept fixed at the DFT-derived values and only nonstructural parameters were adjusted to achieve best overall correspondence with experiment. In this way, phase (ii) is identified as $RuO_2(110)$, an assignment that is confirmed by its single-domain micro-LEED pattern and diffraction imaging in LEEM. Phase (iii) also shows specular $I(V)$ characteristics that are clearly distinct from any of the oxygen adlayer phases, i.e., simulating the spectra requires invoking subsurface oxygen. A qualitative overall match is obtained with the structure of a floating trilayer (O-Ru-O-O) surface oxide,[7] the primary difference being a sharp decrease in the measured intensity above 15 eV, which can be explained by the decreasing angular acceptance of the LEEM

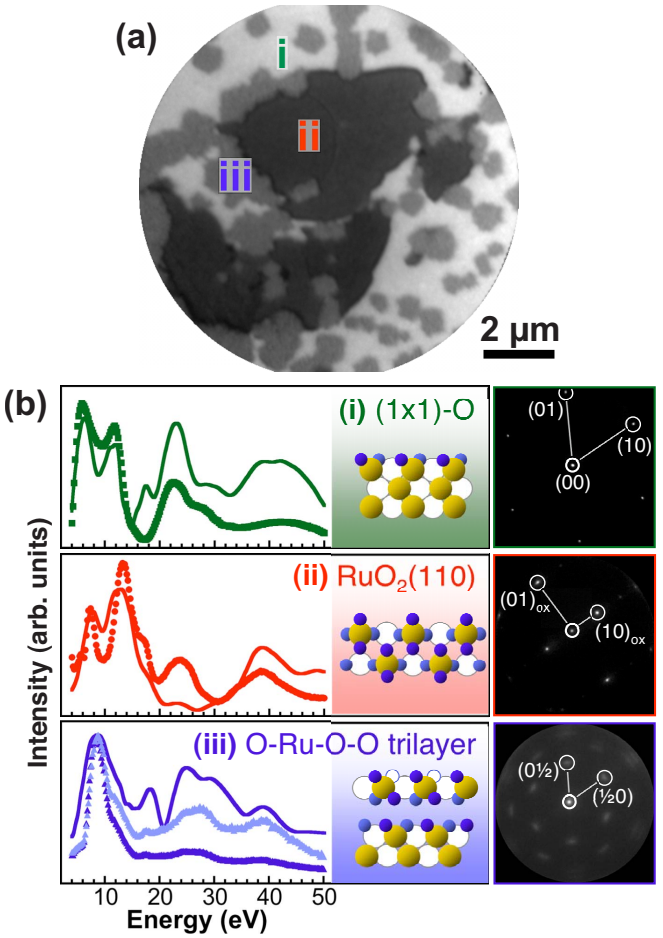

FIG. 1. (Color online) (a) LEEM image (V=9.6 eV) of Ru(0001) oxidized by exposure to 760 L NO_2 at 790 K. (b) Comparison of measured local $I(V)$ spectra (symbols) with LEED theory (Ref. 5) (lines) for DFT-optimized structures (Ref. 7) shown schematically. Light blue symbols for (iii) are experimental data corrected for the energy-dependent transmission of the LEEM optics. Right: selected-area micro-LEED patterns (V=55 eV) from pure phases (i), (ii), and (iii). Lines indicate primitive vectors in reciprocal space.

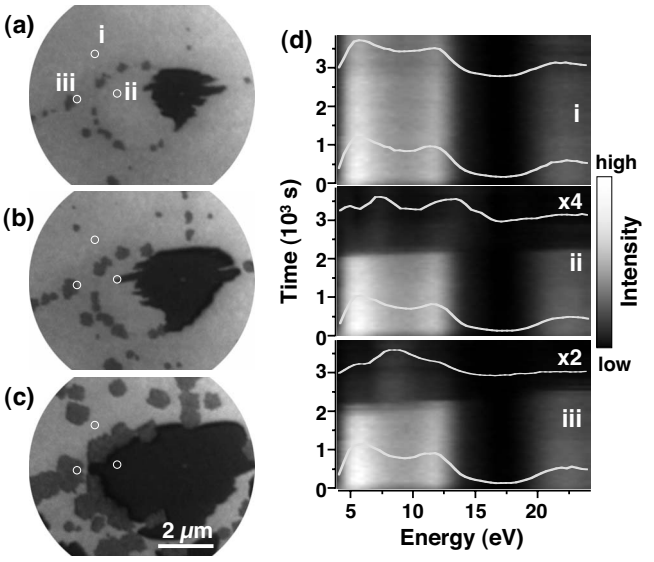

FIG. 2. [(a)–(c)] Time-lapse LEEM images (V=8.4 eV) of Ru(0001) oxidation in NO_2 ($p=2\times10^{-7}$ torr; T=790 K). Exposures: (a) 1600, (b) 2215, and (c) 3625 s. (d) Local time-dependent $I(V)$ characteristics at three points initially in the (1×1)-O phase (a) whose final state after long NO_2 exposure (c) is the O-adlayer (i), $RuO_2(110)$ (ii), and the surface oxide (iii), respectively. Initial and final $I(V)$ curves are shown as white lines; time-dependent spectra are given in grayscale.

electron optics at higher energies for structures exhibiting considerable disorder. Instead of a (1×1) periodicity, as expected for an ideal O-Ru-O-O trilayer,[7] micro-LEED on phase (iii) shows a sixfold symmetric (2×2)-like diffraction pattern with in-plane lattice parameters and crystallographic orientation similar to the Ru(0001) substrate, even under oxygen-rich conditions where a sharp (1×1)-O structure ensues in adjacent adlayer domains. Based on IV-LEEM and micro-LEED, we tentatively associate phase (iii) with a disordered trilayerlike surface oxide, whose O and Ru content is below the saturation concentration of an ideal trilayer structure.[7] An O-deficient structure could avoid the large lattice deformations induced by O incorporation into tetrahedral sites,[2] thereby lowering the overall strain energy and causing the surface oxide to become stable when integrated as a finite domain on Ru(0001).

An O-Ru-O-O trilayer was predicted to play a key role as a transition state between Ru(0001)-(1×1)-O and $RuO_2(110)$.[6] Yet, our observations[10] challenge this prediction. Although a disordered trilayerlike surface oxide nucleates first and its boundary can serve as a nucleation center for $RuO_2(110)$, the two structures grow simultaneously with increasing NO_2 dose, as shown by time-lapse $I(V)$ spectra extracted from IV-LEEM oxidation movies (Fig. 2).

At point (i) where none of the oxygen-rich phases form, the spectrum remains that of the (1×1)-O phase during the entire NO_2 exposure. At points traversed by the growth front of one of the oxygen-rich domains, the (1×1)-O characteristic gives way to a different spectrum during oxidation. Position (iii) shows an abrupt transition from the initial (1×1)-O phase to the surface oxide. Similarly, the local spectrum at point (ii) switches abruptly from the (1×1)-O to the $RuO_2(110)$ characteristics without intermediary spectral features of the surface oxide or any other structure with distinct specular $I(V)$ characteristics. We conclude that the disordered surface oxide and $RuO_2(110)$ are manifestations of *independent competing oxidation pathways* at coverages $\Theta_O > 1$ ML and have similar stability over a range of oxygen coverage at finite temperatures. Indeed, during prolonged NO_2 exposure at high temperatures (810 K) we observe the conversion of the thin $RuO_2(110)$ into the surface oxide.[10]

Overall, our experiments provide two key advances in understanding the initial oxidation of Ru(0001). First, we show that in addition to the $RuO_2(110)$ thin-film oxide a disordered surface oxide forms during oxidation beyond the (1×1)-O adlayer phase, in accordance with interpretations of post-growth local core-level photoemission spectra.[12] While a full structural analysis of this phase is beyond the scope of this paper, the (00) $I(V)$ spectrum of the surface oxide appears consistent with a trilayerlike O-Ru-O stacking.

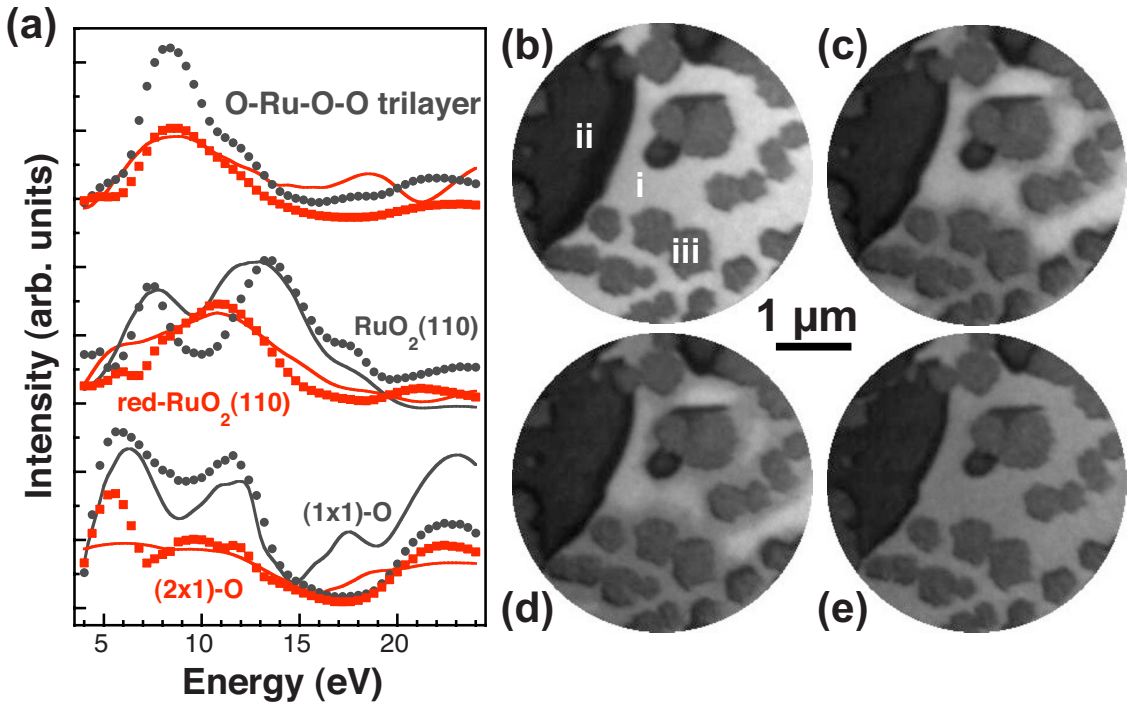

FIG. 3. (Color online) (a) $I(V)$ spectra of the different surface structures on oxidized Ru(0001) before (circles) and after (squares) exposure to 830 L CO at $T=550$ K. Symbols: measurement; lines, LEED calculations for trial structures, as labeled. [(b)–(e)] LEEM images ($V=7.2$ eV) showing the reduction in CO ($p=2\times10^{-7}$ torr; $T=550$ K) of oxidized Ru(0001). (i): O-adlayer; (ii): $RuO_2(110)$; and (iii): surface oxide. CO exposures: (b) 1.6, (c) 183, (d) 285, and (e) 476 L.

Micro-LEED exhibits a local (2×2)-like periodicity with in-plane lattice parameters slightly differing from the underlying Ru(0001) bulk, in accord with a lower O content than an ideal (1×1)-reconstructed trilayer assumed in DFT calculations.[6] Second, our time-resolved observations under reaction conditions disprove the accepted concept that a distinct surface oxide acts as a metastable precursor[6,12] to the RuO_2 thin-film oxide. Instead, a surface oxide coexists with $RuO_2(110)$ domains over a wide range of temperature and gas phase conditions.

III. CATALYSIS ON OXIDIZED Ru(0001)

The accepted mechanism of CO oxidation on Ru(0001) assumes $RuO_2(110)$ as the catalytically active phase generated under oxidizing conditions.[13] Strikingly, CO oxidation catalysis is also reported for Ru(0001) surfaces oxidized at temperatures low enough that the growth of RuO_2 is suppressed,[12] indicating the existence of a second catalytically active oxygen-rich phase. Recently, it has been argued that Ru(0001)-(1×1)-O should be the primary catalytically active phase,[14] which has sparked renewed controversy and illustrates a perhaps unforeseen complexity of this model catalyst system.

The structural heterogeneity of oxidized Ru(0001) observed here may hold the key to resolving this puzzle and shows the limitations of determining catalytic activity without taking into account the detailed near-surface structure of the catalyst. In addition to the different intrinsic activities of coexisting phases, a heterogeneous surface offers the intriguing possibility of *cooperative effects*, such as enhanced reactivity at domain boundaries[15] or the spillover of adsorbates between domains, which can induce catalytic activity on surface phases that would be *inactive in isolation*. We have used *IV*-LEEM to probe the reactivity of individual nanoscale domains and to explore spill-over effects.

Oxidation catalysis on transition-metal oxides frequently follows a Mars–Van Krevelen mechanism[16] in which a reactant molecule (CO) adsorbs on the catalyst, reacts with surface oxygen, and desorbs (as CO_2). This process generates an O vacancy, which is subsequently filled by dissociative adsorption of O_2 from the gas phase to complete the catalytic cycle. The preferred approach for studying such reactions by microscopy is to separate the reduction of the catalyst (in CO) from its reoxidation (in O_2)[17] so as to map the surface modifications induced in these half cycles.

IV-LEEM during exposure of oxidized Ru(0001) to CO shows that the oxygen-rich phases—$RuO_2(110)$ and surface oxide—rapidly and uniformly react with CO, converting to structures identified by comparing local $I(V)$ spectra with simulations [Fig. 3(a)]. Extended CO exposure reduces the rutile $RuO_2(110)$ by generating bridging oxygen vacancies.[13] The $I(V)$ characteristic of the surface oxide remains qualitatively unchanged apart from a uniform decrease in the overall intensity suggesting that CO exposure removes near-surface oxygen without significantly altering the average disordered structure. For very high CO doses, finally, both oxygen-rich phases are reduced completely to Ru(0001)-(1×1)-O. The initial reduction of the (1×1)-O adlayer phase is shown in the LEEM sequence of Fig. 3(b) ($V=7.2$ eV). Its reduction to the (2×1)-O structure (Θ_O

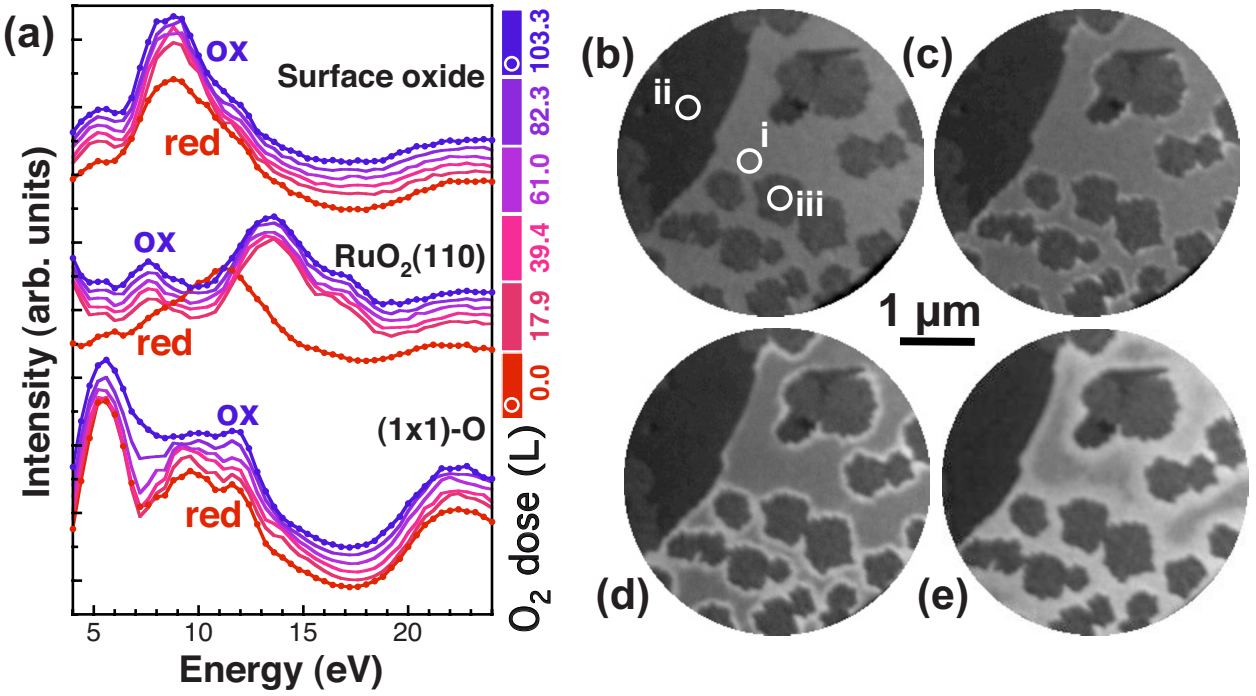

FIG. 4. (Color online) (a) Local time-dependent $I(V)$ spectra during exposure to O_2 at 550 K. [(b)–(e)] LEEM (V=7.2 eV) during reoxidation in O_2 ($p=2\times10^{-7}$ torr; T=550 K) of the reduced surface (Fig. 3). (i) O-adlayer, (ii) $RuO_2(110)$, and (iii) surface oxide. O_2 exposures: (b) 8.7, (c) 30.4, (d) 62.7, and (e) 94.4 L. Circles indicate points where the local $I(V)$ spectra shown in (a) were obtained.

=0.5 ML, Ref. 18) is very slow and is initiated near the boundaries of adjacent domains of the surface oxide (iii). In the immediate vicinity of the surface oxide, the uniformly bright surface (i) with $I(V)$ characteristic of the (1×1)-O phase develops dark bands whose local $I(V)$ spectra are consistent with calculated and early experimental[19] $I(V)$ spectra of a (2×1)-O structure. With increasing CO exposure, the (2×1)-O signature spreads as a diffuse reduction front to the domain center. In contrast, RuO_2 boundaries (ii) do not promote the reduction of Ru(0001)-(1×1)-O by CO.

Microscopy during the reoxidation of the reduced surface (Fig. 4) shows that $RuO_2(110)$ and surface oxide domains very rapidly regenerate when exposed to O_2. Time-dependent $I(V)$ spectra of isolated (2×1)-O areas again show a much slower oxygen uptake. Analogous to the behavior under reducing conditions, reoxidation occurs at higher rates in the vicinity of the surface oxide (iii). Here, the uniformly dark (2×1)-O surface (i) develops bright bands due to the restoration of a higher surface O coverage [Figs. 4(b)–4(e)], as shown by local $I(V)$ spectra [Fig. 4(a)]. With increasing O_2 dose these bands widen continuously, i.e., the reoxidized zone gradually spreads over the entire O-adlayer domains.

Our results on surface oxidation and catalysis on Ru(0001) provide a coherent picture that can resolve the long-standing (and recently rekindled[14]) controversy on the nature of the oxygen-rich phases in this system and their catalytic activity. At the initial stages of Ru(0001) oxidation beyond 1 ML oxygen coverage, a structurally and chemically disordered trilayerlike surface oxide and a RuO_2 thin-film oxide form as coexisting surface phases. Our experiments show that both structures are easily reduced (in CO) and reoxidized (in O_2), and hence have high *intrinsic* catalytic activity for CO oxidation. The CO and O_2 adsorptions on the surface oxide should be enhanced by a large population of adsorption sites due to its disordered structure, in contrast to the expected low reactivity of an ideal (1×1)-O terminated trilayer. On the Ru(0001)-(1×1)-O surface, *IV*-LEEM during consecutive exposure to CO and O_2 shows a low catalytic activity of isolated adlayer areas, orders of magnitude smaller than the other oxygen-rich structures. Yet, on the heterogeneous oxidized surface the adlayer phase shows signs of catalytic activity, which is entirely due to *cooperative effects* in the presence of the neighboring surface oxide domains. The reduction of the (1×1)-O surface is initiated by adsorption of CO close to the surface oxide boundaries and subsequent (slow) reaction with oxygen atoms from the (1×1)-O phase leaving behind oxygen vacancies, which in turn provide adsorption sites for further CO molecules. Stronger binding of the surface oxygen at lower Θ_O (Ref. 11) stabilizes these already reduced areas. Hence, the remaining (1×1)-O phase is reduced preferentially and the further reduction sweeps as a reaction front toward the center of the adlayer domains.

The reoxidation of the (2×1)-O phase also occurs cooperatively with the surface oxide phase. Assuming a high dissociative sticking coefficient of O_2 on the surface oxide and taking the well-known low sticking coefficient on the O-adlayer[20] into account, the most efficient pathway for reoxidation of the adlayer involves spillover of atomic oxygen from adjacent surface oxide domains. Surprisingly, spillover from $RuO_2(110)$, which also easily dissociates O_2, is not seen, suggesting a hindered diffusion of atomic O from RuO_2. While spill-over effects are often observed for oxide supported nanoparticle catalysts, our results highlight the

need of considering such cooperative effects in describing catalysis on heterogeneous metal surfaces, such as oxidized Ru(0001).

IV. CONCLUSIONS

The methodology used here to study Ru(0001) oxidation and catalysis establishes a general framework for analyzing evolving heterogeneous surfaces under reaction conditions. With the ability of performing structural fingerprinting as a function of temperature and gas pressure, *IV*-LEEM can provide a direct experimental window to complex structural transformations of catalytic surface systems, complementing recently developed first-principles statistical mechanics calculations.[21]

ACKNOWLEDGMENTS

We acknowledge P. Zahl for technical support, and R.Q. Hwang and E. Sutter for stimulating discussions. Work performed under the auspices of the U.S. Department of Energy under Contract No. DE-AC02-98CH1-886.

[1] For a recent review, see K. Reuter, in *Nanocatalysis*, edited by U. Heiz and U. Landman (Springer, New York, 2006).
[2] M. Todorova, W. X. Li, M. V. Ganduglia-Pirovano, C. Stampfl, K. Reuter, and M. Scheffler, Phys. Rev. Lett. **89**, 096103 (2002).
[3] J. B. Pendry, *Low Energy Electron Diffraction* (Academic, New York, 1974).
[4] A. K. Schmid, W. Swiech, C. S. Rastomjee, B. Rausenberger, W. Engel, E. Zeitler, and A. M. Bradshaw, Surf. Sci. **331-333**, 225 (1995).
[5] V. Blum and K. Heinz, Comput. Phys. Commun. **134**, 392 (2001).
[6] K. Reuter, C. Stampfl, M. V. Ganduglia-Pirovano, and M. Scheffler, Chem. Phys. Lett. **352**, 311 (2002).
[7] K. Reuter, M. V. Ganduglia-Pirovano, C. Stampfl, and M. Scheffler, Phys. Rev. B **65**, 165403 (2002).
[8] J. Gustafson, A. Mikkelsen, M. Borg, E. Lundgren, L. Köhler, G. Kresse, M. Schmid, P. Varga, J. Yuhara, X. Torrelles, C. Quirós, and J. N. Andersen, Phys. Rev. Lett. **92**, 126102 (2004).
[9] Under these conditions larger continuous domains of the different phases are generated, ideal for structural fingerprinting. Lower temperature ($\geq$600 K) or higher NO_2 pressure produce domains with the same spectroscopic signatures but higher density and smaller size.
[10] See EPAPS Document No. E-PRBMDO-78-103836 for an *IV*-LEEM movie of Ru(0001) oxidation. For more information on EPAPS, see http://www.aip.org/pubservs/epaps.html.
[11] C. Stampfl, S. Schwegmann, H. Over, M. Scheffler, and G. Ertl, Phys. Rev. Lett. **77**, 3371 (1996).
[12] R. Blume, H. Niehus, H. Conrad, A. Böttcher, L. Aballe, L. Gregoriatti, A. Barinov, and M. Kiskinova, J. Phys. Chem. B **109**, 14052 (2005); R. Blume, M. Havecker, S. Zafeiratos, D. Teschner, E. Kleimenov, A. Knop-Gericke, R. Schlögl, A. Barinov, P. Dudin, and M. Kiskinova, J. Catal. **239**, 354 (2006).
[13] H. Over, Y. D. Kim, A. P. Seitsonen, S. Wendt, E. Lundgren, M. Schmid, P. Varga, A. Morgante, and G. Ertl, Science **287**, 1474 (2000).
[14] D. W. Goodman, C. H. F. Peden, and M. S. Chen, Surf. Sci. **601**, L124 (2007).
[15] W. X. Li and B. Hammer, Chem. Phys. Lett. **409**, 1 (2005).
[16] P. Mars and D. W. van Krevelen, Chem. Eng. Sci., Special Supplement **3**, 41 (1954).
[17] Observations of catalysis in oxygen-rich CO/O_2 mixtures have been performed as well and show the same phenomena as the sequential reduction and reoxidation.
[18] H. Pfnür, G. Held, M. Lindroos, and D. Menzel, Surf. Sci. **220**, 43 (1989).
[19] H. Pfnür, M. Lindroos, and D. Menzel, Surf. Sci. **248**, 1 (1991).
[20] H. Over and M. Muhler, Prog. Surf. Sci. **72**, 3 (2003), and references therein.
[21] K. Reuter, D. Frenkel, and M. Scheffler, Phys. Rev. Lett. **93**, 116105 (2004).